Methods, fluxes and sources of gas-phase alkyl nitrates in the coastal air

Alin C. Dirtu[a,b], Anna J. Buczyńska[a], Ana F.L. Godoi[c], Rodrigo Favoreto[a], László Bencs[a,d,*], Sanja S. Potgieter-Vermaak[e,f], Ricardo H.M. Godoi[c], René Van Grieken[a], Luc Van Vaeck[a]

[a] Department of Chemistry, University of Antwerp (UA), Universiteitsplein 1, 2610 Antwerp, Belgium
[b] Department of Inorganic and Analytical Chemistry, University "Al. I. Cuza" of Iassy,700506 Iassy, Romania
[c] Department of Environmental Engineering, Federal University of Paraná (UFPR), Curitiba, Paraná, Brazil
[d] Institute for Solid State Physics and Optics, Wigner Research Centre for Physics, Hungarian Academy of Sciences, POB. 49, H-1525 Budapest, Hungary
[e] Division of Chemistry & Environmental Science, Manchester Metropolitan University, Chester Street, Manchester, M1 5GD, United Kingdom
[f] School of Chemistry, University of the Witwatersrand, Private Bag X3, PO Wits, 2050, South Africa

[*] Corresponding author (Tel.: +36 1 392 2222/1684; Fax: +36 1 392 2223; e-mail: bencs.laszlo@wigner.mta.hu)

Abstract – The daily and seasonal atmospheric concentrations, deposition fluxes and emission sources of a couple of C3-C9 gaseous alkyl nitrates (ANs) were studied over the Belgian coast (De Haan) at the Southern North Sea. An adapted/further developed sampler design for the low- and high-volume air-sampling, optimized sample extraction and clean-up, as well as identification and quantification of ANs in air samples by means of gas chromatography mass spectrometry, are reported. The air levels of the study ΣANs ranged from 0.03 to 85 pptv, consisting primarily of the nitro-butane and nitro-pentane isomers. Air-mass backward trajectories were calculated by the Hybrid Single-Particle Lagrangian Integrated Trajectory (HYSPLIT) model, to determine the influence of main air masses on AN air levels. The shorter chain ANs have been the most abundant in the Atlantic/Channel/United Kingdom air masses, while the longer chain ANs in continental air. The overall mean N-fluxes of the ANs were slightly higher for summer than for winter-spring, although their contributions to the total nitrogen flux were low. In winter/spring the study ANs were correlated to air HNO_2 levels, while in summer the shorter chain ANs were related to precipitation. Source apportionment by means of principal component analysis indicated that the most of the gas phase ANs could be attributed to traffic/combustion, secondary photochemical formation and biomass burning, although marine sources may also have been present and a contributing factor.

Keywords Organic nitrates, N-nutrients, High volume air sampler, Electron ionization ion-trap GC-MS, Breakthrough volume, Source identification

Introduction

Photochemical processes and oxidant chemistry in the atmosphere are influenced by nitrogen oxides, ozone, hydrocarbons (HCs), and organosulphur compounds (Crutzen 1979; Logan et al. 1981; Liu et al. 1983; Altshuller 1986; Toon et al. 1987). Amongst these gases, alkyl nitrates (ANs or $RONO_2$) are of particular interest, especially, within the ozone/nitrogen oxide system, because their formation and degradation play an important role in tropospheric ozone production (Atkinson et al. 1982; Singh 1987; Luke and Dickerson 1988; Roberts and Fajer 1989; Roberts 1990). The formation of alkyl nitrates via oxidation of parent hydrocarbons has been a well-known atmospheric mechanism since the 1970s (Darnall et al. 1976). As ozone and organic nitrates are formed through the same reaction, monitoring the air concentrations of organic nitrates can provide information on the role of various peroxy radicals in photochemical ozone formation (Flocke et al. 1991). Besides photochemical AN formation, oceanic sources of ANs have been identified for the past decades (Walega et al. 1992; Atlas et al. 1993; Chuck et al. 2002; Ballschmiter 2002). Moreover, biomass burning has been observed as a major point source of C_1-C_4 alkyl nitrates, although these emissions are expected to insignificantly impact global reactive nitrogen levels (Simpson et al. 2002). The primary alkyl nitrate sinks are reported to be photolysis and reaction with hydroxyl radicals (Roberts 1990; Clemitshaw et al. 1997; Talukdar et al. 1997; Aschmann et al. 2011; Russo et al. 2013), although the influence of photochemical AN loss decreases with increasing atomic number (Clemitshaw et al. 1997, Talukdar et al. 1997).

Several studies have been devoted to investigate the temporal (daily, seasonal) variations and geographical distributions of alkyl nitrates (e.g., Atlas 1988; Simpson et al. 2006). Airborne measurements have shown alkyl and multifunctional nitrates (ΣANs) to be a significant fraction (~10 %) of NOy in a number of different chemical regimes (Perring et al. 2010). They have drawn three important conclusions: (1) correlations of ΣANs with odd-oxygen (O_x) indicate a stronger role for ΣANs in the photochemistry of Mexico City than is expected on the base of current photochemical mechanisms, (2) ΣAN formation suppresses peak O_3 production rates by as high as 40 % near Mexico City and (3) ΣANs play a significant role in the transport of NO_y from Mexico City to the Gulf Region. Alkyl nitrates have also been proven to form in air pollution originating from oil spill accidents (Neuman et al. 2012).

The atmospheric nitrogen-input, especially at coastal regions, triggers increasing interest in the scientific community. Specifically, atmospheric nitrogen fluxes, in terms of inorganic and organic nitrogen deposition, are important to be assessed by experimental and model approaches, in order to get an insight into their contribution to eutrophication processes at coastal regions.

The low air concentrations of ANs and the complexity of the atmospheric system in terms of organic gas phase and aerosol components with a wide range of polarity make sampling, direct detection and quantification of ANs in the ambient air a challenging task. Sampling of gas phase ANs in air has been performed in several ways, using Tenax adsorption columns (Luxenhofer et al. 1994; Fischer et al. 2000, 2002), a combination of Tenax cartridges and polyurethane (PU) foam (Luxenhofer et al. 1994), silicagel and PU foam (Luxenhofer et al. 1996), silicagel and Tenax (Schneider et al. 1998; Schneider and Ballschmiter 1999), or even charcoal (Atlas and Schauffler 1991; De Kock and Anderson 1994). Simpson et al. (2006) pre-concentrated trace gases from air samples by passing ~1.5 L of canister air through a stainless steel tube filled with 1/8-inch diameter glass beads and immersed in liquid nitrogen. A mass flow controller with a maximum allowed flow of 500 mL min^{-1} controlled the trapping process. The trace gases were re-volatilized using a hot water bath and then reproducibly split into five streams for detection as follows below.

Generally, organic nitrates have been measured by high-resolution (HR) gas chromatography (GC) with electron capture detection (ECD) (De Kock and Anderson 1994; Moschonas and Glavas 2000; Glavas 2001; Glavas and Moschonas 2001; Fischer et al. 2002; Simpson et al. 2006; Russo et al. 2010; Zhang et al. 2013) and a combination of GC-ECD and GC-MS (Luxenhofer et al. 1994; Luxenhofer et al. 1996; Schneider et al. 1998; Schneider and Ballschmiter 1999; Fisher et al. 2000).

Both traditional injections of a concentrated extract (De Kock and Anderson 1994; Luxenhofer et al. 1994, 1996; Schneider et al. 1998; Schneider and Ballschmiter 1999), as well as thermal desorption from adsorption traps and cryo-trapping have been applied in the analysis of ANs (Fischer et al. 2000; Moschanos and Glavas 2000; Fischer et al. 2002). Nevertheless, pre-separation of ANs is still a critical step of the chemical analysis. For this purpose, diverse procedures have been described, such as adsorption chromatography on silicagel (Luxenhofer et al. 1996; Schneider and Ballschmiter 1999), or normal-phase high-performance liquid chromatography with an organonitrate stationary phase (Fischer et al. 2000).

Within the framework of a study aiming at the characterization of nitrogen-containing organic compounds in the marine environment, it appeared to be necessary to develop a sensitive and robust analytical procedure for the determination of ANs, particularly, with the application of GC-MS, it being available in the laboratory of the present research team. In this paper, an adapted and a further developed design of an air sampler for the low and high volume collection of gaseous and aerosol phase atmospheric ANs is reported together with optimized extraction, clean-up, and GC-MS identification and quantification. The preparation of suitable standards of various AN compounds for method calibration is discussed. The daily and seasonal air levels and deposition fluxes of gas phase ANs together with the identification of possible emission sources of these compounds are also reported.

Experimental

Sampling and weather data collection

A common high volume (HiVol) sampler has been redesigned for the combined collection of aerosol and gas phase components of the ambient air using either a low or high capacity gas adsorption trap (see Supplementary Information). Daily (24-hour) atmospheric air samples were taken four days a week (by starting at 14:00 GMT) at a small coastal research/meteorological station of the Flanders Marine Institute (VLIZ), located in De Haan, Belgium (51°17′12.77″ N, 3°03′39.53″ E, 6 m a.m.s.l.), during two weeks in August 2005 and five months (February-April and June-July) in 2006. Wind direction (WD), wind speed (WS), precipitation, relative humidity (RH), air pressure (P_{air}) and air temperature (T_{air}) were monitored and logged by a computer every minute on each day of the sampling campaigns.

For collecting atmospheric PM, a glass fibre filter (Whatmann GF 25) was fitted into the HiVol sampler. Gas phase sampling with low capacity adsorption traps was achieved using 2 g of 60-80 mesh Tenax-TA® (Buchem BV, Apeldoorn, the Netherlands) in each of the four tubes of the sampler. The ANs were pre-extracted from the adsorbent with acetone in a Soxhlet-column under reflux for 8 h. A total volume of less than 20 m^3 was sampled at a flow rate of 3 m^3 h^{-1} over the four traps. Alternatively, the high capacity adsorption trap was filled with 100 g of 35-70 mesh, silicagel (Sigma Aldrich NV/SA, Bornem, Belgium) for capturing the gas phase components. The silicagel was washed before sampling with a 4:1 (v/v) mixture of pentane-dichloromethane and activated in an electric oven at 160 °C for 24 hours. For

each sample, an air volume of typically 250 m^3 was pumped through at a flow rate of 10 m^3 h^{-1}. The chemicals applied in this work were of analytical grade or better, if not stated otherwise. Ultrapure MilliQ water and organic solvents were applied for cleaning, dissolution and dilution (see Supplementary Information).

Synthesis of alkyl nitrate standards

Apart from the commercially available isopropyl and isobutyl nitrate (99 % purity, Aldrich Chem. Co., Steinheim, Germany), the other studied ANs were synthesized in the UA-laboratory to produce high-purity standards for the calibration of the GC-MS method. The corresponding alkyl halides (i.e., iodides for methyl and 2-butyl nitrates and corresponding bromide for other ANs synthesized) were dissolved in ~10^{-3} mol L^{-1} acetonitrile, then mixed with a solution of silver nitrate in acetonitrile, containing a two-fold excess of the equivalent amount needed in the reaction, and stirred for 24 h in the dark at room temperature (RT) (Ferris et al. 1953; Luxenhofer et al. 1994). During reaction, ANs segregated as a distinct layer at the top of the aqueous solution, which phases were separated in an extraction funnel. The extract, containing the ANs, was washed with water, dried on Na_2SO_4. Afterwards the ANs were recovered from the drying agent with dichloromethane. The reaction yields for these syntheses were higher than 95%. The nomenclature used in this paper for ANs is according to Schneider and Ballschmiter (1996) and Fischer et al. (2002), for instance, 1C3 and 2C5 stand for 1-butyl nitrate and 2-pentyl nitrate, respectively (see Table S1 in Supplementary Information).

Extraction and clean-up procedures

For the recovery of the gas phase AN compounds from Tenax TA® adsorbents, Soxhlet extraction with 150 mL of acetone and pentane (8 h for each) was applied. The excess solvent was evaporated at RT under a gentle nitrogen flow to obtain a sample volume of 0.5 mL. Further sample clean-up utilized a glass column with an internal diameter (ID) of 10 mm, containing 4 g Florisil (100-200 mesh, Fluka, Buchs, Switzerland), activated before use at 120 ºC for 12 h. Pentane was used as an eluent and the fraction between 9 and 27 mL was kept for analysis. Subsequently, the sample volume was reduced to about 0.5 mL under a nitrogen stream at RT and the samples were stored at -20 ºC in a deep-freezer prior to injection onto the GC-MS.

The organic compounds were eluted from the silicagel samples with a 400 mL aliquot of 4:1 (v/v) mixture of pentane-dichloromethane in a water cooled glass column (25.6 cm length, 4 cm ID) (Schneider and Ballschmiter 1999). The extract was concentrated to 150 μL at RT under a gentle nitrogen flow. The 2-fluoro-toluene was used as a recovery and an internal standard for the optimization steps and for the GC-MS analysis.

GC-MS separation, detection and quantitation

All measurements were performed on a Varian Model Saturn 2000 GC-MS (Varian Inc., Lake Forest, CA, USA) equipped with ion-trap and electron ionization (EI) units. A VF-1ms capillary column (100% dimethylpolysiloxane, Varian Inc.) with a length of 30 m, an ID of 0.25 mm and a film thickness of 1 μm was used with a helium flow rate of 1 cm^3 min^{-1}. Sample aliquots of 1 μL were injected splitless. The temperatures of the injector, the transfer line and the ion-trap were set at 250, 220 and 240 ºC, respectively. The temperature program for the GC oven was as follows: 40 ºC for 5.8 min, increase to 51 ºC with 3 ºC min^{-1} and hold for 2 min, increase to 75 ºC with 3.5 ºC min^{-1} and hold for 3.5 min, increase to 96 ºC with 5 ºC min^{-1} and hold for 2.5 min and increase with 10 ºC min^{-1} to 260 ºC and hold for 8.13 min. A total chromatographic cycle of 51 min provided the best separation for all AN isomers detected in the air samples. The mass selective detection, following EI of ANs was based on the formation of the intense NO_2^+ fragment at *m/z* 46. Analytical performance data of the developed GC-MS method are listed in Table S2. The LODs obtained with this method (0.001-0.005 pptv) are sufficiently low to quantify the study ANs in most of the samples on the condition of an air volume of 250 m^3 is collected.

Calculation of air-mass trajectories and alkyl nitrate fluxes

Single-tracks and ensembles of air-mass backward trajectories (BWTs) were calculated for the start and end time of each day of the sampling by the Hybrid Single-Particle Lagrangian Integrated Trajectory (HYSPLIT) Model (Draxler and Rolph 2003; Rolph 2003). The BWTs were applied to determine the influence of main air-masses, i.e., the Atlantic Ocean, the North Sea, and the continent, on the air levels of ANs. Typical ensembles of BWTs representing the main air-masses are depicted on Fig. 1.

The literature has not yet reported dry deposition velocities (v_d) for individual alkyl nitrates over sea surfaces. Therefore, to estimate of the AN-fluxes, a generalized literature (model) value on organic nitrate deposition for sea water surfaces (0.027 cm/s) was selected (Hertel et al. 1995). It is to be noted that the model and experimental v_d values for over-land dry deposition are around an order of magnitude higher, e.g., for organic nitrates: 0.12 cm/s (Hertel et al. 1995), for $MeONO_2$: 0.13 cm/s (Russo et al. 2010), which corresponds to ~4.5-times higher N-fluxes of ANs over land, implying the same air AN levels and weather conditions. The 24 h N-flux data of individual ANs were assorted according to the origin of main air-masses on the base of the single-track BWTs, i.e., Atlantic/Channel, North Sea, continental, or mixed. From these data, the average N-fluxes, their fluctuations, expressed as the standard deviation (SD), and the total N-contributions were calculated.

Statistical methods

The method of bivariate correlation analysis with the Pearson's correlation coefficient (r) at a two-tailed significance level (p) was used with the IBM® SPSS® Statistics software package (version 20). Since there is no data in the literature on PCA of alkyl nitrates, their daily concentrations together with the data on inorganic gases and ionic species of PM sampled concurrently (Bencs et al. 2009; Horemans et al. 2009) were processed using PCA, in order to assist the recognition of contributing factors/emission sources. For PCA, Varimax rotation and Kaiser normalization were applied as described in the literature (Costello and Osborne 2005). Principal components (PCs) having eigenvalues higher than one in the component data set were retained, i.e., those which could still be classified as plausible emission sources on the basis of the component loadings. In PCs, species having loadings above 0.7 and below 0.4 were characterized as high and low, respectively. Species having PC loading of less than 0.4 were considered either not be related to the other species or were explored in an additional PC (Costello and Osborne 2005). Reference data on source apportionment published in a comprehensive review (Viana et al. 2008) were also utilized for comparison.

Results and discussion

Sampling methodology

The use of adsorption columns is the most common method to collect organic compounds from the gas phase (e.g., Atlas and Schauffler 1991). A critical parameter to be considered is the breakthrough volume of the gas adsorption system. On one hand, the sampled volume should be as high as possible to facilitate the detection of air-components present at ultra-trace levels. On the other hand, overloading of the gas adsorption trap may result in partial losses due to evaporation. It is a common practice to determine the limiting volume by connecting two adsorption columns in series (Atlas and Schauffler 1991; Luxenhofer and Ballschmiter 1994; Schneider and Ballschmiter 1999). However, in this case, the limit of detection (LOD) of the analytical method determines the extent, to which the breakthrough volume of the first adsorption column must be exceeded.

As an alternative approach, isothermal adsorption chromatography has been applied in the present study. For this purpose, a conventional glass column was packed with an accurately weighed amount of the adsorbent. The retention volume in isothermal elution on a GC-ECD system was determined at various temperatures. Plotting the logarithms of the corrected retention volumes as a function of the reciprocal temperature gives a linear relationship, which can be extrapolated with good accuracy to derive a realistic value for the breakthrough volume. The breakthrough volumes from 1C3 to 1C7 for 2 g Tenax TA® were 0.5 to 300 m^3, respectively, and for 1C3 on 100 g silicagel, the value was 310 m^3. For this adsorbent, only the breakthrough volume for the most volatile AN was determined, otherwise, the retention time would have become too long for AN-analogues of longer carbon chains at the maximal allowable column temperature. Specifically, whenever the accurate sampling of C3 is aimed at, the sampling volume should be lower than 0.26 and 3.1 m^3 per g Tenax TA® and silicagel, respectively. Besides the substantially higher retention capacity of silicagel, it is more cost effective than Tenax TA®. Thus it can be advantageously used even in large adsorption traps without any need of adsorbent recovery after extraction and analysis. Therefore, for ambient air sampling, 100 g silicagel was applied in this study.

Daily and seasonal variations in the air levels of alkyl nitrates

In summer, 11 ANs have been identified and quantified, but only 8 of them were detected in winter-spring (Table 1). The mean air concentrations and the relative abundance of individual AN analogues/isomers have shown seasonal differences. The air levels of individual ANs in the late summer, winter/spring, and midsummer seasons ranged from 0.001-0.005 pptv (below LOD) to 78 pptv (Table 1), with median concentrations of 0.07, 0.08, and 0.11 pptv, respectively. These median air concentrations rather represent a marine/coastal background. These concentrations are generally lower than those reported in the literature for marine air (De Kock and Anderson 1994), though the sampling for the latter was performed at least a decade earlier. The study ΣAN fraction consists primarily of the 1C4, 2C4, 3C5 and 2C5 compounds.

The daily trends of the ΣAN concentrations and the corresponding (average) weather data are depicted on Fig. 3. As it can be seen, the ΣAN level exhibits high day-to-day variation, as a result of the influence of various air masses and meteorological conditions. The high extent of rainfall, high RH, and/or high wind speed caused a decrease in the air concentrations of ΣANs. The higher air temperature also resulted in drop in the ΣAN air levels. This could be expected on the base of the literature, since under higher incoming solar radiation, the atmosphere works more effectively as a sink of ANs, due to more photolysis and an increased rate of AN decomposition (Talukdar et al. 1997).

Seasonality of ANs at the coastal site can be observed too, in terms of their usually higher levels during winter-spring than summer (Fig. 3). The occasionally occurring high peaks of ΣANs in summer have also been observed, which is most probably due to the prevailing continental air masses, transporting high pollution load to the coastal site. Another factor is assumed to be the higher local traffic density during summer at and around the seaside resort as compared to winter/spring.

Estimation of alkyl nitrate fluxes

Late summer season in 2005

The highest average daily deposition was observed for 3C5 and for Atlantic/Channel/UK air-masses (0.47 ng N m^{-2} day^{-1}), followed by lower values for the mixed North Sea/continental air-masses (0.23 ng N m^{-2} day^{-1}), but around the LOD (0.12 ng N m^{-2} day^{-1}) for North Sea air-masses. The contribution of 2C4 was also significant for Atlantic/Channel/UK air-masses (i.e., 0.45 ng N m^{-2} day^{-1}),

whereas lower contributions were found for 1C3, 1C4, 2C5, 1C5, 3C6, 2C6, 1C6, and 1C8 ANs with similar fluxes (0.02-0.09 ng N m^{-2} day^{-1}). For the North Sea influenced air masses, the contributions from 2C4 and 2C5 were found to be very significant, with average deposition values of 0.14 and 0.12 ng N m^{-2} day^{-1}, respectively. Moreover, 1C4, 1C5, 3C6, 2C6, and 1C6 also contributed to the flux, with 0.03-0.07 ng N m^{-2} day^{-1}. Under mixed continental-North Sea influence, the contribution was significant for 1C4, 3C5, 2C5, and 1C9 compounds, with deposition rates of 0.1, 0.23, 0.15, and 0.08 ng N m^{-2} day, respectively. The 1C5, 3C6, 2C6, 1C6, 1C7, and 1C8contributed lower to the N-flux, each with around 0.025-0.06 ng N m^{-2} day^{-1}.

The average fluxes of ANs for the Atlantic/Channel/UK, North Sea and the mixed continental-North Sea air masses were found to be 1.5, 0.72, and 0.96 ng N m^{-2} day^{-1}, corresponding to an overall AN flux of 1.1 ng N m^{-2} day^{-1} for this short late summer period. In late summer, the contribution of shorter chain ANs prevails from Oceanic air-masses, while for continental and North Sea air-masses, the longer chain ANs also contribute to the N-flux of the study ANs (Fig. 4).

Late winter/spring season in 2006

In the late winter/spring period, a high average daily flux of 3C5 has also been found for all the three main air-masses, ranging from 1.1 to 2.5 ng N m^{-2} day^{-1}. For the Atlantic/Channel/UK air-masses, the average contribution of 3C5 was 1.2 ng N m^{-2} day^{-1}, i.e. ~60 % of the total flux of the study ANs (Fig. 4). Lower contributions were found for 2C5 (0.26 ng N m^{-2} day^{-1}), 2C6 with 0.12 ng N m^{-2} day^{-1}, whereas the fluxes of 1C4, 1C5, 1C6, 1C8, and 1C9 were much lower, i.e., 0.05, 0.08, 0.08, 0.03, and 0.03 ng N m^{-2} day^{-1}, respectively.

For continental air-masses, fairly intensive average fluxes of 2C4, 3C5, 2C5, 2C6, 1C6, and 1C7, i.e., 2.3, 1.1, 0.4, 0.8, 1.4, and 1.1 ng N m^{-2} day^{-1}, respectively, have been observed. The 1C8 and 1C9 only contributed with negligibly low fluxes of 0.07 and 0.03 ng N m^{-2} day^{-1}, respectively. For air-masses, arriving from the North Sea, the flux of 3C5 was extremely high, i.e., with an average value of 2.5 ng N m^{-2} day^{-1}, corresponding to ~70 % of the total average N-flux of the detected ANs. The other ANs, characteristic for this air-mass, were 2C5, 1C5, 2C6, 1C6 and 1C8 with medium N-fluxes, ranging between 0.13-0.24 ng N m^{-2} day^{-1}. Negligibly low fluxes of 1C3, 1C4, 2C4, 1C7 and 1C9 were found with values of 0.01-0.05 ng N m^{-2} day^{-1}.

The average fluxes of ANs for the Atlantic/Channel/UK, continental and North Sea air-masses were found to be 2.0, 7.4, and 3.6 ng N m^{-2} day^{-1}, corresponding to an overall AN-flux of 3.8 ng N m^{-2} day^{-1} for winter/spring. It can be concluded that the highest contribution of AN-fluxes originate from air-masses approaching from the continent, whereas the contributions of Atlantic and the North Sea air masses are lower by 73% and 51%, respectively. The contribution of shorter chain ANs is dominant from marine air-masses, while for continental air-masses, the longer chain ANs also considerably contribute to the N-fluxes of the study ANs (Fig. 4).

Midsummer season in 2006

In midsummer, similarly to the late summer period, the AN-fluxes were the most significant from the Atlantic/Channel/UK air-masses and again from 3C5, but also 1C4 with average values of 0.9 and 2.1 ng N m^{-2} day^{-1}. The 2C5 and 1C8 compounds also contributed to the N-flux, but to a much lower extent than the former ANs, i.e., with depositions around 0.01-0.12 ng N m^{-2} day^{-1}. The fluxes of 2C6, 1C5, 1C6, and 1C7 were negligibly low, ranging between 0.01-0.06 ng N m^{-2} day^{-1}, respectively.

For continental air masses, the daily average fluxes of 1C4, 3C5 and 1C8 were found to be the most significant contributors, i.e., 0.26, 0.77 and 0.54 ng N m^{-2} day^{-1}, respectively. The fluxes of 1C5, 2C6, 1C6, and 1C7 were lower, ranging between 0.08-0.11 ng N m^{-2} day^{-1}. For North Sea air-masses, the flux of 3C5 was the most decisive with an average value of 0.9 ng N m^{-2} day^{-1}. The 1C4, 2C5, 1C5, and 2C6 contributed to the N-flux to a low and varying extent, i.e., 0.21, 0.15, 0.34, 0.28, while the fluxes of 1C6, 1C7, 1C8 and 1C9 were similar, i.e., each ~0.5, ng N m^{-2} day^{-1}.

The average fluxes of ANs for the Atlantic/Channel/UK, continental and North Sea air-masses were found to be 3.6, 2.2, and 4.1 ng N m^{-2} day^{-1}, corresponding to an overall average AN-flux of 3.2 ng N m^{-2} day^{-1}. For midsummer, generally the contribution of lower chain ANs prevails for Atlantic and continental air-masses, while for North Sea air-masses, the longer chain ANs also similarly contribute to the N-flux of the study ΣANs, which is similar observation to that made for late summer (Fig. 4).

Source apportionment

Correlation analysis

The results for winter-spring and summer show several correlations between ANs, the inorganic species sampled concurrently and the corresponding daily weather data (Table S3). Furthermore, seasonal trends can be observed too. In winter-spring, especially 1C4 is highly correlated with HNO_2, fine-Cl^-, 3C5, 1C5, 2C6, 1C7 and 1C9 air levels, but anti-correlated with T_{air} and RH. Apparently, 3C5 showed similar correlations, also for medium-NH_4^+, but anti-correlated with coarse-NH_4^+ and WS. The 2C5 was correlated to medium&fine-$NH_4^+/NO_3^-/SO_4^{2-}/K^+$ and WS, but anti-correlated to T_{air}. The 1C5 was also highly correlated with fine-Cl^-, 1C4, 3C5, 2C6, 1C7 and 1C9. It is notable that 2C6 and 1C6 are correlated, also with HNO_2 and medium-$NH_4^+/NO_3^-/SO_4^{2-}$, which shows that these compounds may take part in secondary reactions with aerosols, likely via photochemical ways. The resulting HNO_2 may assist in secondary aerosol formation and/or growth. The 2C6 is also related to rain-NO_3^- and P_{air}. The 1C8 was correlated to coarse-NH_4^+, while 1C9 was anti-correlated to medium-NO_3^-.

In summer, a higher number of between species correlations are experienced compared to the winter-spring season. For instance, 1C4 was strongly correlated with 3C5, 2C6, 1C6, 1C7, 1C9, medium-$NH_4^+/SO_4^{2-}/K^+$, and fine-Mg^{2+}. The 3C5 showed the same correlation with the latter inorganic species, but in terms of ANs, it was only correlated with 2C5 and 1C4. The 2C5 was correlated with medium/fine-$NO_3^-/SO_4^{2-}/Na^+$, fine-Cl^-, and also with 2C6, 1C6, 1C7 and RH, but anti-correlated with 3C5, T_{air} and WS. These results point to a lower extent of 2C5 formation at higher T_{air} (corresponding to higher incoming solar radiation flux), and/or intensified photochemical decomposition of this compound. The 1C5 and 2C6 correlated well with each other and longer chain alkyl nitrates. Shorter chain alkyl nitrates (C3-C5) were generally correlated with medium/fine fractions of $NH_4^+/SO_4^{2-}/K^+$, which points towards sources of biomass burning. The longer chain alkyl nitrates were related with each other and coarse K^+. Interestingly, 1C4 and 3C5 correlated well with precipitation in summer.

Principal component analysis

For winter-spring, several PCs have been found (Table S4). PC1 has high loadings of coarse-$Cl^-/Mg^{2+}/Ca^{2+}$, medium loadings for coarse Na^+, SO_4^{2-}, NO_3^-, and for medium-sized Na^+ and Cl^- too, corresponding to sea spray aerosol component. Similar loadings have been found for sea salt components sampled over Amsterdam

(Valius et al. 2005), which is also reported to be common for this type of aerosol (Viana et al. 2008). PC2 has high loadings of medium/fine K^+, fine NH_4^+/SO_4^{2-}, medium loadings of 2C5 and fine NO_3^-, and low loading for 1C9. Biomass burning has been reported as a source of short chain alkyl nitrates (Simpson et al. 2002). PC2 accounts for emissions from local combustion, most likely vehicular traffic and/or biomass burning. PC3 has high loadings for coarse $K^+/NH_4^+/SO_4^{2-}$, medium loadings of coarse Na^+/NO_3^-, and fine Na^+/Cl^-, which demonstrates coagulated secondary aerosols, combined likely with freshly formed sea salt. When including the weather data in PCA, this component was also closely related to WS and T_{air}, which supports long-range transport. Interestingly, PC4 has high loadings of the longer chain alkyl nitrates, like 1C6, 2C6 and 1C7, and a low loading of 3C5, while PC6 has high loadings of the shorter chain ANs, i.e., 1C4 and 1C5, a low loading of 2C5, and medium loadings of 3C5 and 1C9. It is presumed that PC4 accounts for the photochemical formation of alkyl nitrates, likely, through secondary processes in the troposphere, as reported by Atkinson et al. (1982). This is also supported by low loadings of HNO_2, HNO_3 and medium-$NH_4^+/NO_3^-/SO_4^{2-}$, received in this PC. On the other hand, PC6 may suggest a marine source of alkyl nitrates, which is presumed to be on the base of a weak correlation to sea salt components. PC5 has high loadings of medium-sized $NH_4^+/NO_3^-/SO_4^{2-}/Mg^{2+}$ and medium loadings for HNO_2 and Ca^{2+}, which points towards diesel emissions. PC7 has medium loadings for HNO_3 and medium-size Na^+, corresponding to local combustion. PC8 has medium loadings of HNO_3 and coarse/medium Ca^{2+}, corresponding to local background pollution. PC 9 has high loadings for NH_3 and medium loadings for HNO_2. This factor represents emissions originating from extensive animal farming activities over nearby agricultural areas of West Flanders (Bencs et al. 2008).

For the summer season in 2006 (Table S5), PC1 has high loadings of most alkyl nitrates (i.e., 1C5, 2C5, 1C6, 2C6, 1C7, 1C8, and 1C9), and a medium loading for HNO_3. These longer chain alkyl nitrates seem to have the same source in summer, i.e., secondary processes, most likely through photochemical conversion of the corresponding radicals of parent hydrocarbons (Atkinson et al. 1982). PC2 has high loadings for several species of fine PM ($Na^+/Cl^-/NO_3^-/K^+/Mg^{2+}/Ca^{2+}$) and medium loadings for NH_4^+/SO_4^{2-}, which points toward freshly formed secondary aerosols , possibly through fresh, finely dispersed sea spray particles as nucleation centers (Horemans et al. 2009). PC3 has high loadings for coarse NH_4^+, Na^+, K^+, Mg^{2+} and

458 Ca^{2+}, which shows soil dust resuspension. PC4 is characterized by high loadings of
459 medium-sized Na^{+}/Cl^{-}, which clearly points to sea spray origin, as mentioned above.
460 PC5 is characterized by high loadings of 1C4, 3C5, medium-sized K^{+}, medium
461 loadings of medium-sized NH_4^{+}/SO_4^{2-}, and low loadings of fine Mg^{2+}/SO_4^{2-}, which
462 factor most possibly reflects the contribution of biomass burning activities at nearby
463 agricultural fields. PC6 has a high loading of medium-sized NO_3^{-}, and a medium
464 loading of HNO_2, medium/fine-NH_4^{+}/SO_4^{2-} and coarse NO_3^{-}, corresponding to
465 secondary aerosol. PC7 has high loadings of coarse SO_4^{2-}/Cl^{-} and medium loading of
466 NO_3^{-}, which factor corresponds likely to regional/coastal background. PC9 has high
467 loadings for NH_3 and medium loadings for HNO_2, which represents emissions from
468 animal farming activities as noted above.
469
470 **Conclusions**
471 The redesigned HiVol sampler allows the simultaneous collection of aerosol
472 and gas phase components of the ambient air using either a low, or high capacity gas
473 adsorption trap. This sampling and the developed analytical methodology exhibits the
474 accurate determination of gas phase ANs (e.g., those with 3-9 carbon atoms) from
475 ambient air samples with minimal pre-separation using the species selectivity and
476 high sensitivity of EI-GC-MS.
477 The N-fluxes of the study ΣANs at the coastal sampling site are slightly more
478 pronounced in summer than in winter-spring, although their contribution to the total
479 (wet+dry) nitrogen flux is still considered to be low (cf. Bencs et al. 2009). Higher
480 ΣAN-fluxes have been observed from the continent and the North Sea in winter/spring
481 compared to those from Atlantic/Channel/UK air-masses, while in summer the fluxes
482 from the latter air-mass were also increased. In summer, most of the shorter chain
483 gaseous ANs are correlated with precipitation, while in winter-spring, the study
484 compounds are related with the HNO_2 content of air. Some ANs were anti-correlated
485 with air temperature, suggesting a photochemical sink.
486 Occasional high peaks of ANs, originating from continental air pollution, have
487 also been experienced in summer over De Haan. These were likely due to higher local
488 traffic density and more frequency of continentally influenced air during summer near
489 this seaside resort as compared to winter/spring. It is important to note, however, that
490 these effects can mask the regular seasonality of ANs, reported in the literature, i.e.,

the peak and the lowest AN air levels in the cold and warm season, respectively (e.g., Swanson et al. 2003).

The principal component analysis showed at least 3-4 sources of gaseous alkyl nitrates at the coastal study site (depending on the season), the most important being local combustion (e.g., diesel emissions of vehicular traffic/shipping), secondary photochemical formation from parent hydrocarbons, and biomass burning. On the other hand, one cannot rule out the marine origin of a part of the shorter chain alkyl nitrates (e.g., 1C4, 2C5), they being evidently correlated to certain sea salt aerosol components.

Acknowledgment

One of the authors (Alin C. Dirtu) acknowledges an EC grant within Marie Curie program HPMT-CT-2001-00310. The authors are thankful for the technical support provided by Jan Van Loock (UA), André Cattrijsse, Frank Broucke, and Francisco Hernandez (VLIZ). The authors gratefully acknowledge the NOAA Air Resources Laboratory (ARL) for the provision of the HYSPLIT transport and dispersion model and/or READY website (http://www.arl.noaa.gov/ready.html) used in this publication.

References

Altshuller, A.P. (1986). The role of nitrogen oxides in nonurban ozone formation in the planetary boundary layer over N. America, W. Europe and adjacent areas of ocean. *Atmospheric Environment*, 20(2), 245-268.

Aschmann, S.M., Tuazon, E.C., Arey, J., & Atkinson, R. (2011). Products of the OH radical-initiated reactions of 2-propyl nitrate, 3-methyl-2-butyl nitrate and 3-methyl-2-pentyl nitrate. *Atmospheric Environment*, 45(9), 1695-1701.

Atkinson, R., Aschmann, S.M., Carter, W.P.L., Winer, A.M., & Pitts Jr., J.M. (1982). Alkyl nitrate formation from NO_x-air photooxidations of C_2-C_8 n-alkanes. *Journal of Physical Chemistry*, 86(23), 4563-4569.

Atlas, E. (1988). Evidence for ≥C3 alkyl nitrates in rural and remote atmospheres. *Nature* 331, 426-428.

Atlas, E., & Schauffler, S. (1991). Analysis of alkyl nitrates and selected halocarbons in the ambient atmosphere using a charcoal preconcentration technique. *Environmental Science & Technology*, 25(1), 61-67.

Atlas, E., Pollock, W., Greenberg, J., Heidt, L., & Thompson, A.M. (1993). Alkyl nitrates, nonmethane hydrocarbons, and halocarbon gases over the equatorial Pacific Ocean during SAGA 3. *Journal of Geophysical Research*, 98, 16,933-16,949.

Ballschmiter, K. (2002). A marine source for alkyl nitrates, *Science*, 297(5584), 1127-1128.

Bencs, L., Ravindra, K., de Hoog, J., Rasoazanany, E.O., Deutsch, F., Bleux, N., Berghmans, P., Roekens, E., Krata, A., Van Grieken, R. (2008) Mass and ionic composition of atmospheric fine particles over Belgium and their relation with gaseous air pollutants. *Journal of Environmental Monitoring*, 10(10) 1148-1157.

Bencs, L., Krata, A., Horemans, B., Buczyńska, A.J., Dirtu, A.C., Godoi, A.F.L., Godoi, R.H.M., Potgieter-Vermaak, S., & Van Grieken, R. (2009). Atmospheric nitrogen fluxes at the Belgian coast: 2004-2006. *Atmospheric Environment*, 43(24), 3786-3798.

Clemitshaw, K.C., Williams, J., Rattigan, O.V., Shallcross, D.E., Law, K.S., & Cox, R.A. (1997). Gas-phase ultraviolet absorption cross-sections and atmospheric lifetimes of several C_2-C_5 alkyl nitrates. *Journal of Photochemistry and Photobiology A: Chemistry*, 102(2-3), 117-126.

Costello, A.B., & Osborne, J.W. (2005). Best practices in exploratory factor analysis: four recommendations for getting the most from your analysis. *Practical Assessment Research & Evaluation*, 10(7), 1-9.

Crutzen, P.J. (1979). The role of NO and NO_2 in the chemistry of the troposphere and stratosphere. *Annual Review of Earth and Planetary Sciences*, 7, 443-472.

Chuck, A.L., Turner, S.M., & Liss, P.S. (2002). Direct evidence for a marine source of C_1 and C_2 alkyl nitrates. *Science*, 297(5584), 1151-1154.

Darnall, K.R., Carter, W.P.L., Winer, A.M., Lloyd, A.C., & Pitts, Jr., J.N. (1976). Importance of RO_2 + NO in alkyl nitrate formation from C_4–C_6 alkane photooxidations under simulated atmospheric conditions. *Journal of Physical Chemistry*, 80(17), 1948-1950.

De Kock, A.C., & Anderson, C.R. (1994). The measurement of C_3-C_5 alkyl nitrates at a coastal sampling site in the Southern Hemisphere. *Chemosphere*, 29(2), 299-310.

Draxler, R.R., & Rolph, G.D. (2003). HYSPLIT (HYbrid Single-Particle Lagrangian Integrated Trajectory) Model access via NOAA ARL READY Website (http://www.arl.noaa.gov/ready/hysplit4.html). NOAA Air Resources Laboratory, Silver Spring, MD.

561 Ferris, A.F, McLean, K.W., Marks, I.G., & Emmons, W.D. (1953). Metathetical
562 reactions of silver salts in solution. III. The synthesis of nitrate esters. *Journal of*
563 *the American Chemical Society*, 75(16), 4078-4082.
564 Fischer, R.G., Kastler, J., & Ballschmiter, K. (2000). Levels and pattern of alkyl
565 nitrates, multifunctional alkyl nitrates and halocarbons in the air over the Atlantic
566 Ocean. *Journal of Geophysical Research: Atmospheres*, 105(D11), 14473-14494.
567 Fischer, R., Weller, R., Jacobi, H.W., & Ballschmiter, K. (2002). Levels and pattern
568 of volatile organic nitrates and halocarbons in the air at Neumayer Station (70^{o} S),
569 Antarctica. *Chemosphere*, 48(2), 981-992.
570 Flocke, F., Volz-Thomas, A., & Kley, D. (1991). Measurements of alkyl nitrates in
571 rural and polluted air masses. *Atmospheric Environment, Part A: General Topics*,
572 25(9), 1951-1960.
573 Glavas, S. (2001). Analysis of C_2-C_4 peroxyacyl nitrates and C_1-C_5 alkyl nitrates with
574 a non-polar capillary column. *Journal of Chromatography A*, 915(1-2), 271-274.
575 Glavas, S., & Moschonas, N. (2001). Determination of PAN, PPN, P*n*BN and selected
576 pentyl nitrates in Athens, Greece. *Atmospheric Environment*, 35(32), 5467-5475.
577 Hertel, O., Christensen, J., Runge, E.H., Asman, W.A.H., Berkowicz, R., Hovmand,
578 M.F., & Hov, Ø. (1995). Development and testing of a new variable scale air-
579 pollution model – ACDEP. *Atmospheric Environment*, 29(11), 1267-1290.
580 Horemans, B., Krata, A., Buczynska, A.J., Dirtu, A.C., Van Meel, K., Van Grieken,
581 R., & Bencs, L. (2009). Major ionic species in size-segregated aerosols and
582 associated gaseous pollutants at a coastal site on the Belgian North Sea. *Journal of*
583 *Environmental Monitoring*, 11(3), 670-677.
584 Liu, S.C., McFarland, M., Kley, D., Zafiriou, O., & Huebert, B. (1983). Tropospheric
585 NO_x and O_3 budgets in the equatorial Pacific. *Journal of Geophysical Research:*
586 *Oceans*, 88(2), 1360-1368.
587 Logan, J.A., Prather, M.J., Wofsy, S.C., & McElroy, M.B. (1981). Tropospheric
588 chemistry: A global perspective. *Journal of Geophysical Research: Oceans*,
589 86(C8), 7210-7254.
590 Luke, W.T., & Dickerson, R.R. (1988). Direct measurements of the photolysis rate
591 coefficient of ethyl nitrate. *Geophysical Research Letters*, 15(11), 1181-1184.
592 Luxenhofer, O., & Ballschmiter, K. (1994). C_4-C_{14} alkyl nitrates as organic trace
593 compounds in air. *Fresenius' Journal of Analytical Chemistry*, 350(6), 395-402.
594 Luxenhofer, O., Schneider, E., & Ballschmiter, K. (1994). Separation, detection and
595 occurrence of (C2-C8)-alkyl- and phenyl-alkyl nitrates as trace compounds in clean
596 and polluted air. *Fresenius' Journal of Analytical Chemistry*, 350(6), 384-394.
597 Luxenhofer, O., Schneider, M., Dambach, M., & Ballschmiter, K. (1996).
598 Semivolatile long chain of C6-C17 alkyl nitrates as trace compounds in air.
599 *Chemosphere*, 33(3), 393-404.
600 Moschonas, N., & Glavas, S. (2000). Simple cryoconcentration technique for the
601 determination of peroxyacyl and alkyl nitrates in the atmosphere. *Journal of*
602 *Chromatography A*, 902(2), 405-411.
603 Neuman, J.A., Aikin, K.C., Atlas, E.L., Blake, D.R., Holloway, J.S., Meinardi, S.,
604 Nowak, J.B., Parrish, D.D., Peischl, J., Perring, A.E., Pollack, I.B., Roberts, J.M.,
605 Ryerson, T.B., & Trainer, M. (2012). Ozone and alkyl nitrate formation from the
606 Deepwater Horizon oil spill atmospheric emissions. *Journal of Geophysical*
607 *Research: Atmospheres*, 117(9), Art. D09305.
608 Perring, A.E., Bertram, T.H., Farmer, D.K., Wooldridge, P.J., Dibb, J., N. J. Blake,
609 N.J., Blake, D.R., Singh, H.B., Fuelberg, H., Diskin, G., Sachse, G., & Cohen R.C.

(2010). The production and persistence of $\Sigma RONO_2$ in the Mexico City plume. *Atmospheric Chemistry and Physics*, 10(15), 7215-7229.
Roberts, J.M., & Fajer, R.W. (1989). UV absorption cross sections of organic nitrates of potential atmospheric importance and estimation of atmospheric lifetimes. *Environmental Science & Technology*, 23(8), 945-951.
Roberts, J.M. (1990). The atmospheric chemistry of organic nitrates. *Atmospheric Environment, Part A: General Topics*, 24(2), 243-287.
Rolph, G.D. (2003). Real-time Environmental Applications and Display System (READY) Website. (http://www.arl.noaa.gov/ready/hysplit4.html). NOAA Air Resources Laboratory, Silver Spring, MD.
Russo, R.S., Zhou, Y., Wingenter, O.W., Frinak, E.K., Mao, H., Talbot, R.W., & Sive, B.C. (2010). Temporal variability, sources, and sinks of C_1-C_5 alkyl nitrates in coastal New England. *Atmospheric Chemistry and Physics*, 10(4), 1865-1883.
Schneider, M., & Ballschmiter, K. (1996). Separation of diastereomeric and enantiomeric alkyl-nitrates – Systematic approach to chiral discrimination on cyclodextrin LIPODEX-D. *Chemistry – A European Journal*, 2(5), 539-544.
Schneider, M., Luxenhofer, O., Deissler, A., & Ballschmiter, K. (1998). C_1-C_{15} alkyl nitrates, benzyl nitrate and bifunctional nitrates: Measurements in California and South Atlantic air and global comparison using C_2Cl_4 and $CHBr_3$ as marker molecules. *Environmental Science & Technology*, 32(20), 3055-3062.
Schneider, M., & Ballschmiter, K. (1999). C_3-C_{14}-alkyl nitrates in remote South Atlantic air. *Chemosphere*, 38(1), 233-244.
Simpson, I.J., Meinardi, S., Blake, D.R., Blake, N.J., Rowland, F.S., Atlas, E., & Flocke, F. (2002). A biomass burning source of C_1–C_4 alkyl nitrates. *Geophysical Research Letters*, 29(24), Art. 2168, 21/1-21/4.
Simpson, I.J., Wang, T., Guo, H., Kwok, Y.H., Flocke, F., Atlas, E., Meinardi, S., Rowland, F.S., & Blake, D.R. (2006). Long term atmospheric measurements of C_1-C_5 alkyl nitrates in the Pearl River Delta region of southeast China. *Atmospheric Environment*, 40(9), 1619-1632.
Singh, H.B. (1987). Reactive nitrogen in the troposphere. *Environmental Science & Technology*, 21(4), 320-327.
Swanson, A.L., Blake, N.J., Atlas, E., Flocke, F., Blake, D.R., & Rowland, F.S. (2003). Seasonal variations of C_2-C_4 nonmethane hydrocarbons and C_1-C_4 alkyl nitrates at the Summit research station in Greenland. *Journal of Geophysical Research*, 108(D2), Art. 4065, 7/1-7/19.
Talukdar, R.K., Burkholder, J.B., Hunter, M., Gilles, M.K., Roberts, J.M., & Ravishankara, A.R. (1997). Atmospheric fate of several alkyl nitrates. Part 2. UV absorption cross-sections and photodissociation quantum yields. *Journal of the Chemical Society, Faraday Transactions*, 93(16), 2797-2805.
Toon, O.B., Kasting, J.F., Turco, R.P., & Liu, S.M. (1987). The sulfur cycle in the marine atmosphere. *Journal of Geophysical Research: Atmospheres*, 92(D1), 943-963.
Vallius, M., Janssen, N.A.H., Heinrich, J., Hoek, G., Ruuskanen, J., Cyrys, J., Van Grieken, R., de Hartog, J.J., Kreyling, W.G., & Pekkanen, J. (2005). Sources and elemental, composition of ambient $PM_{2.5}$ in three European cities. *Science of the Total Environment*, 337(1-3), 147-162.
Viana, M., Kuhlbusch, T.A.J., Querol, X., Alastuey, A., Harrison, R.M., Hopke, P.K., Winiwarter, W., Vallius, M., Szidat, S., Prévôt, A.S.H., Hueglin, C., Bloemen, H., Wåhlin, P., Vecchi, R., Miranda, A.I., Kasper-Giebl, A., Maenhaut, W., &

Hitzenberg, R. (2008). Source apportionment of particulate matter in Europe: A review of methods and results. *Journal of Aerosol Science*, 39(10), 827-849.

Walega, J.G., Ridley, B.A., Madronich, S., Grahek, F.E., Shetter, J.D., Sauvain, T.D., Hahn, C.J., Merrill, J.T., Bodhaine, B.A., & Robinson, E. (1992). Observations of peroxyacetyl nitrate, peroxypropionyl nitrate, methyl nitrate and ozone during the Mauna Loa Observatory Photochemistry Experiment. *Journal of Geophysical Research: Atmospheres*, 97(D10), 10311-10330.

Zhang, G., Mu, Y.J., Liu, J.F., & Mellouki, A. (2013). Direct and simultaneous determination of trace-level carbon tetrachloride, peroxyacetyl nitrate, and peroxypropionyl nitrate using gas chromatography-electron capture detection. *Journal of Chromatography A*, 1266, 110-115.

671 **Figure Captions**

672

673 **Fig. 1** Typical ensembles of air-mass backward trajectories calculated by the
674 HYSPLIT Model, representing (a) Atlantic/Channel/UK, (b) North Sea, and (c)
675 continental air-masses

676

677 **Fig. 2** Mass chromatograms at *m/z* 46 for a reference mixture of alkyl nitrates (IS –
678 internal standard) and mass spectra for 2C4 and 1C9

679

680 **Fig. 3** Daily and seasonal variation of the ΣAN concentration and meteorological
681 parameters (abbreviations for air-masses: C – continental, AC – Atlantic/Channel/UK,
682 and NS – North Sea)

683

684 **Fig. 4** Percent contributions of individual alkyl nitrates to the N-flux of ΣANs from
685 the main air-masses during various seasons

686

687 **Fig. 1.**

688

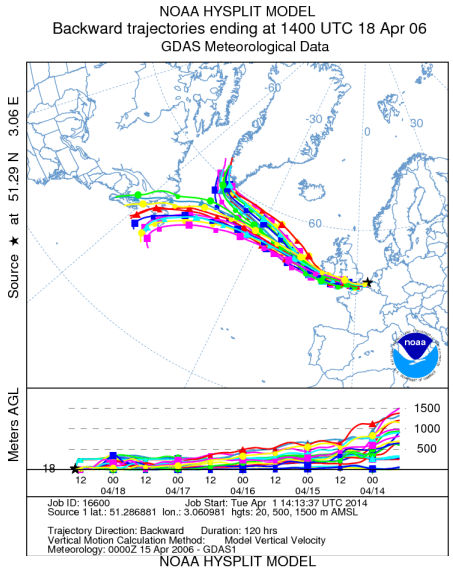

689

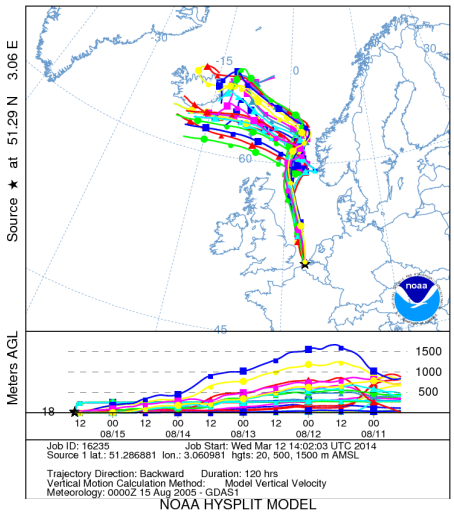

690

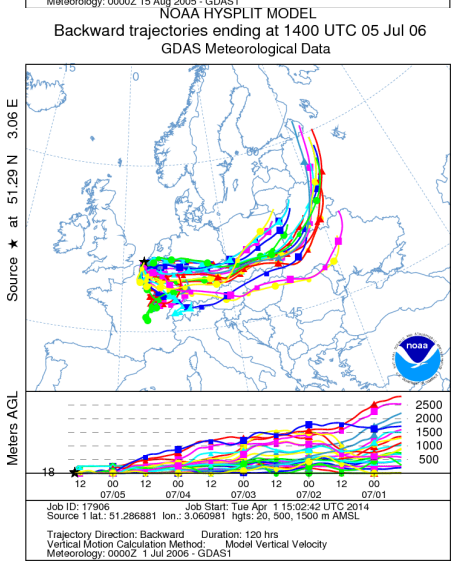

691

Fig. 2.

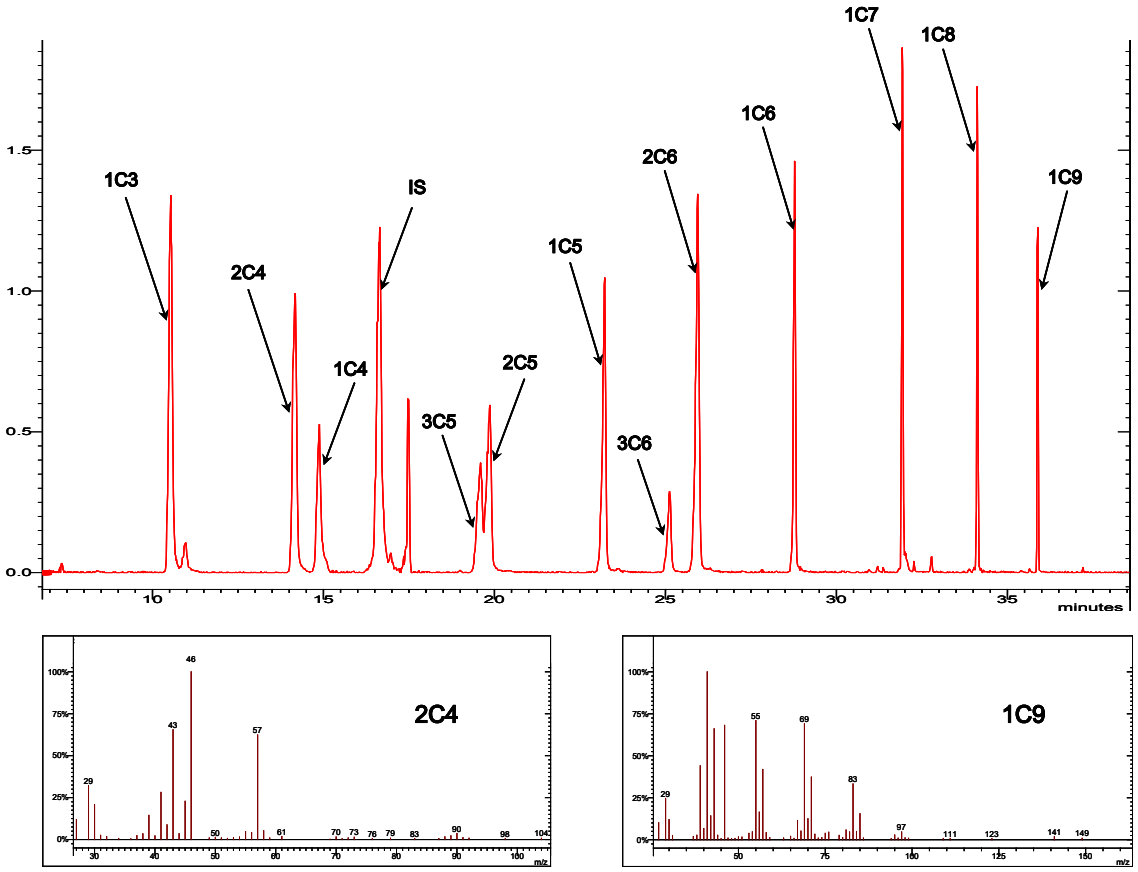
1C3
2C4
1C4
IS
3C5
2C5
1C5
3C6
2C6
1C6
1C7
1C8
1C9
minutes
2C4
1C9

Fig. 3.

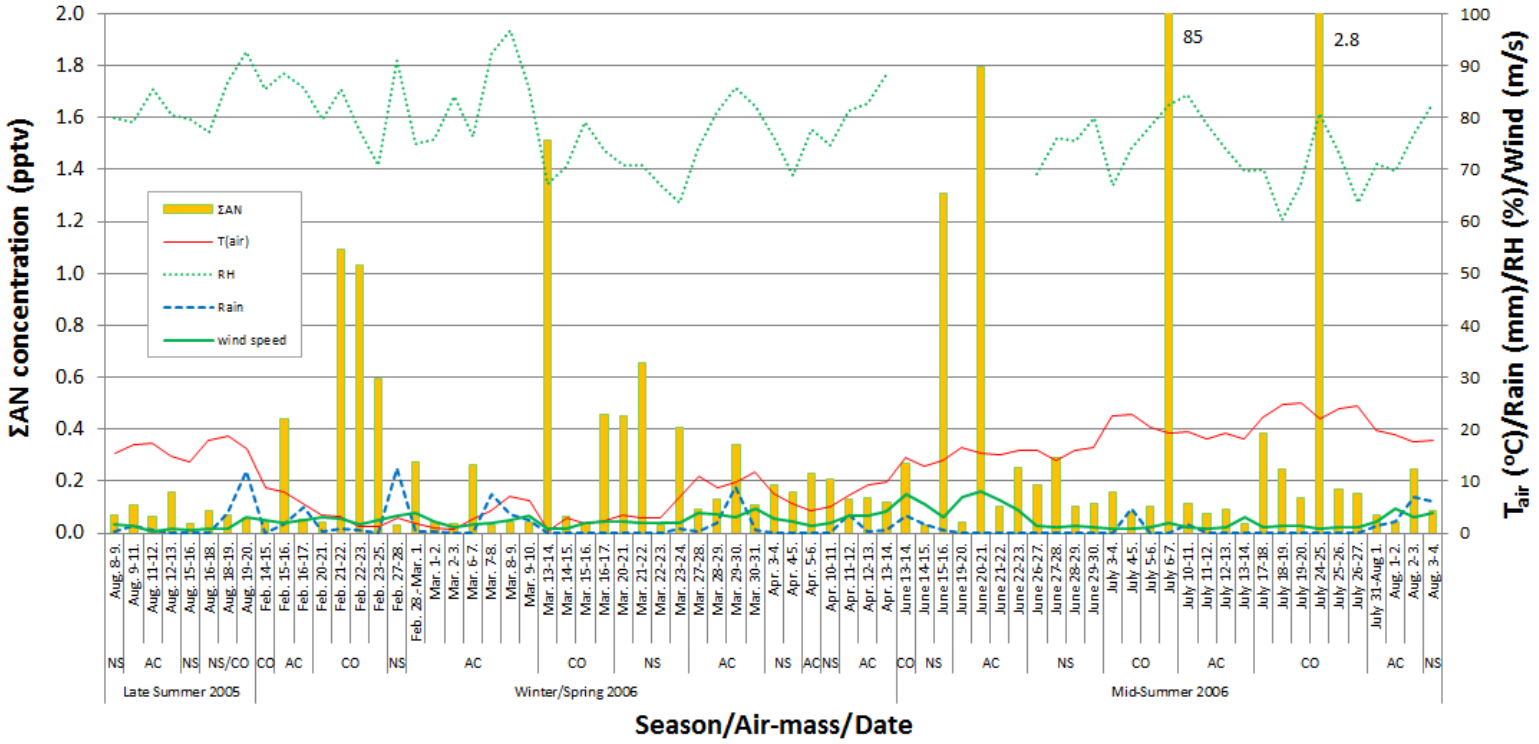
ΣAN concentration (pptv)
Tair (°C)/Rain (mm)/RH (%)/Wind (m/s)
ΣAN
T(air)
RH
Rain
wind speed
85
2.8
Late Summer 2005
Winter/Spring 2006
Mid-Summer 2006
Season/Air-mass/Date

Fig. 4.

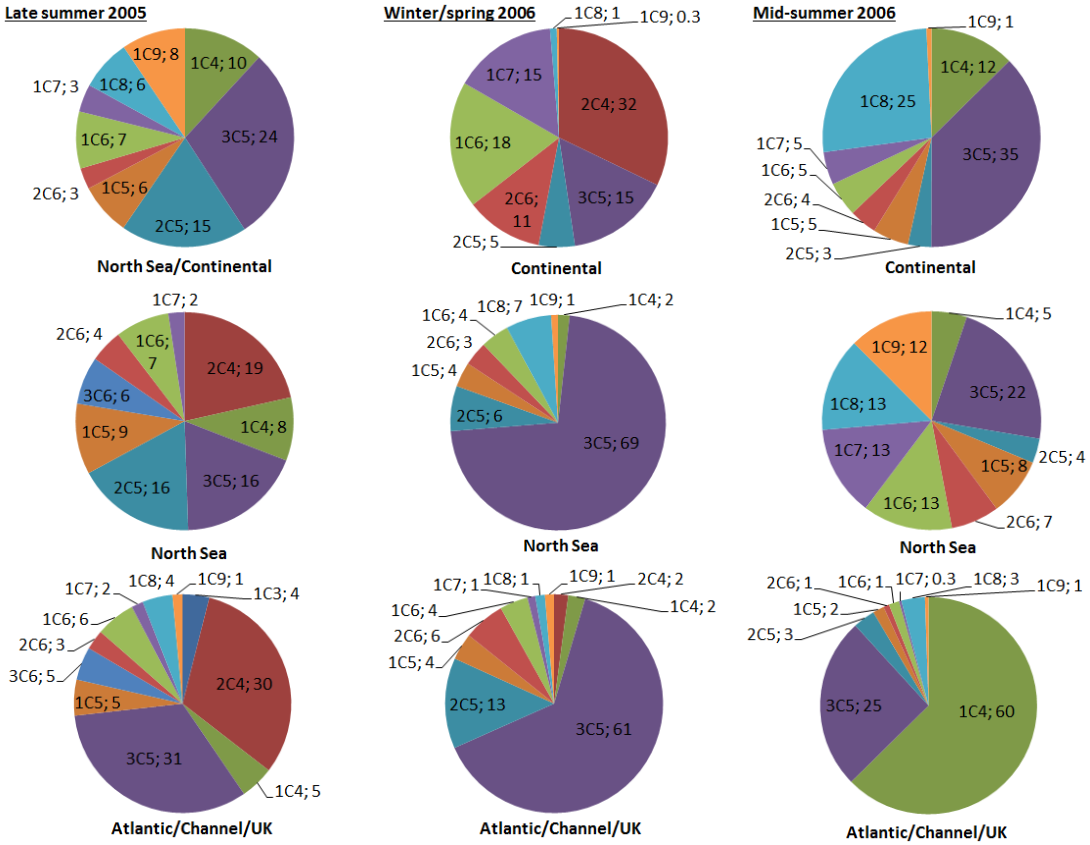
Late summer 2005
1C4; 10
3C5; 24
2C5; 15
1C5; 6
2C6; 3
1C6; 7
1C7; 3
1C8; 6
1C9; 8
North Sea/Continental
Winter/spring 2006
1C8; 1
1C9; 0.3
2C4; 32
3C5; 15
2C5; 5
2C6; 11
1C6; 18
1C7; 15
Continental
Mid-summer 2006
1C9; 1
1C4; 12
3C5; 35
2C5; 3
1C5; 5
2C6; 4
1C6; 5
1C7; 5
1C8; 25
Continental
1C7; 2
2C6; 4
1C6; 7
2C4; 19
3C6; 6
1C4; 8
1C5; 9
2C5; 16
3C5; 16
North Sea
1C6; 4
1C8; 7
1C9; 1
1C4; 2
2C6; 3
1C5; 4
2C5; 6
3C5; 69
North Sea
1C4; 5
1C9; 12
3C5; 22
1C8; 13
2C5; 4
1C7; 13
1C5; 8
1C6; 13
2C6; 7
North Sea
1C7; 2
1C8; 4
1C9; 1
1C3; 4
1C6; 6
2C6; 3
3C6; 5
2C4; 30
1C5; 5
3C5; 31
1C4; 5
Atlantic/Channel/UK
1C7; 1
1C8; 1
1C9; 1
2C4; 2
1C4; 2
1C6; 4
2C6; 6
1C5; 4
2C5; 13
3C5; 61
Atlantic/Channel/UK
2C6; 1
1C6; 1
1C7; 0.3
1C8; 3
1C9; 1
1C5; 2
2C5; 3
3C5; 25
1C4; 60
Atlantic/Channel/UK

Table 1 Atmospheric alkyl nitrate concentrations and detection frequencies in various seasons over De Haan, Belgium

Parameter		Season	Alkyl nitrate concentration (pptv)												
			1C3	**2C4**	**1C4**	**3C5**	**2C5**	**1C5**	**3C6**	**2C6**	**1C6**	**1C7**	**1C8**	**1C9**	**ΣAN**
Median		Late summer 2005	0.005	0.01	0.006	0.014	0.009	0.005	0.004	0.003	0.005	0.002	0.003	0.002	**0.07**
		Winter/spring 2006	n.d.	n.d.	0.003	0.048	0.007	0.002	n.d.	0.003	0.003	0.001	0.002	0.002	**0.08**
		Midsummer 2006	n.d.	n.d.	0.005	0.065	0.008	0.004	n.d.	0.003	0.002	0.001	0.006	0.001	**0.11**
Range	**min**	Late summer 2005	n.d.	0.002	0.003	n.d.	n.d.	0.002	n.d.	n.d.	0.002	n.d.	n.d.	n.d.	**~0.04**
		Winter/spring 2006	n.d.	n.d.	n.d.	n.d.	n.d.	n.d.	n.d.	n.d.	n.d.	n.d.	n.d.	n.d.	**~0.03**
		Midsummer 2006	n.d.	n.d.	n.d.	0.0023	n.d.	n.d.	n.d.	n.d.	n.d.	n.d.	n.d.	n.d.	**~0.03**
	max	Late summer 2005	0.008	0.044	0.011	0.073	0.014	0.008	0.007	0.004	0.01	0.004	0.009	0.008	**0.2**
		Winter/spring 2006	n.d.	1.5	0.013	0.54	0.22	0.035	n.d	0.25	0.38	0.38	0.13	0.008	**3.5**
		Midsummer 2006	n.d	0.007	6.4	78.8	0.042	0.10	n.d.	0.12	0.22	0.25	0.25	0.24	**86.4**
Quartiles	**1st**	Late summer 2005	0.004	0.006	0.004	0.008	0.003	0.004	0.003	0.002	0.004	0.001	0.002	0.001	**0.04**
		Winter/spring 2006	n.d.	n.d.	0.002	0.01	0.004	0.002	n.d.	0.002	0.0013	0.001	0.001	0.001	**0.03**
		Midsummer 2006	n.d.	0.002	0.003	0.037	0.005	0.002	n.d.	0.002	0.0012	0.001	0.002	0.001	**0.06**
	3rd	Late summer 2005	0.005	0.026	0.006	0.027	0.012	0.006	0.006	0.004	0.006	0.003	0.005	0.004	**0.11**
		Winter/spring 2006	n.d.	0.0054	0.005	0.16	0.024	0.004	n.d.	0.019	0.014	0.001	0.002	0.003	**0.25**
		Midsummer 2006	n.d.	0.0053	0.006	0.092	0.009	0.01	n.d.	0.006	0.01	0.002	0.04	0.002	**0.19**
Detection frequency (%)		Late summer 2005	13	50	100	50	38	100	38	75	100	88	50	38	n.a.
		Winter/spring 2006	0	2	8	18	11	6	0	16	14	6	3	4	n.a.
		Midsummer 2006	0	0	38	83	7	41	0	41	41	28	55	10	n.a.

Note: ΣAN –sum of the study alkyl nitrates; n.d. – not detected (i.e, below the LOD of the applied method); n.a. – not applicable.

20

27

SUPPLEMENTARY INFORMATION

"Methods, fluxes and sources of gas-phase alkyl nitrates in the coastal air"

A.C. Dirtu[a,b], A.J. Buczyńska[a], A.F.L. Godoi[c], R. Favoreto[a], L. Bencs[a,d], S.S. Potgieter-Vermaak[e,f], R.H.M. Godoi[c], R. Van Grieken[a], L. Van Vaeck[a]

[a] Department of Chemistry, University of Antwerp (UA), Universiteitsplein 1, B-2610 Antwerp, Belgium
[b] Department of Inorganic and Analytical Chemistry, University "Al. I. Cuza" of Iassy,700506 Iassy, Romania
[c] Department of Environmental Engineering, Federal University of Paraná (UFPR), Curitiba, Paraná, Brazil
[d] Institute for Solid State Physics and Optics, Wigner Research Centre for Physics, Hungarian Academy of Sciences, POB 49, H-1525 Budapest, Hungary
[e] Division of Chemistry & Environmental Science, Manchester Metropolitan University, Chester Street, Manchester, M1 5GD, United Kingdom.
[f] School of Chemistry, University of the Witwatersrand, Private Bag X3, PO Wits, 2050, South Africa

Description of the modified HiVol sampler

A common HiVol sampler has been redesigned for combined collection of aerosol and gas phase components of the ambient air using either a low or high capacity gas adsorption trap. Particular attention has been paid to redesign the shape of the housing to reduce the effects of the changes in the wind direction on sampling, and to improve protection of samples during sample change. Furthermore, a rugged pump system and rotameter control of the sampling rate have been incorporated to ensure reliable and maintenance-free operation over long periods without the need to calibrate the flow rate, as a function of the under-pressure over a calibrated orifice.

The particles are collected on a filter with a diameter of 11 cm in a stainless steel filter holder with separate pressing and tightening rings to avoid filter damage during mounting (Fig. S1). A Viton O-ring is used for sealing. The filter is mounted on the top of a cylindrical manifold with a length of 30 cm and an internal diameter (ID) of 9 cm. The large capacity adsorption trap with an ID of 70 mm and a height of 50 mm can be inserted in the cylinder and is sealed by a Viton O-ring, of which groove is calculated for dynamic sealing. The adsorption trap can take up about 175 cm^3 of adsorbent, corresponding to 100 g of silicagel (35-70 mesh). The cylinder is also fitted with four aspiration tubes for the four low capacity adsorption traps. The tube diameters are calculated to maintain isokinetic sampling to avoid turbulences in the system. The low capacity traps consist of glass tubes (ID: 8 mm, length: 95 mm), mounted in stainless steel protection tubes with the aid of two external O-rings. Screw connections of generous dimensions allow the tubes to be mounted leak-free with finger tightening only. Connections and protection tubes are again sealed by O-rings and the pressing rings are separated from the turning fittings. The exits of the four gas traps are connected to a housing of which the internal design allows combination of the flows into one exit under laminar conditions. The flow through the four gas traps together is measured by a rotameter (RAGH02-D2ST-G161A-PP16, Rota Yokogawa, Wehr, Germany) and directed to another housing, where it is combined with the flow through the main aspiration line at the bottom of the manifold cylinder. Also, here the bottom of the cylinder is conically shaped inside to avoid any turbulence. To

compensate for the hydrodynamic resistance of the gas traps, a 2 inch diameter ball valve is fitted between the manifold and the second connection housing. From that housing, the air flows through a large rotameter (Model RAGH06-D2ST-G471A-PPN45, Rota Yokogawa, Wehr, Germany) to the vacuum pump (max. flow rate 40 m^3 h^{-1}, DT4.40 Becker GmbH, Wuppertal, Germany) with constant flow characteristics over a wide range of low-pressure conditions.

Except the pump, the sampling system is mounted in an aluminum housing (50x50x100cm) with a pyramidal roof (height: 40 cm). The pyramidal shape avoids the asymmetry of the roof section, common for commercial HiVol samplers (with two vertical and two angular surfaces) and thereby avoids the effect of the wind direction on the sampling characteristics. A completely radial symmetry would be ideal, but it complicates construction, and in addition, field studies require easy (de)mounting of the set-up. The sampler is mounted on lightweight rods extending at an angle of 45° with lead-filled supports to ensure stable positioning without the aid of additional means and under stormy wind conditions. The housing has a door and opening section on two opposite sites, so that the sample can be exchanged either side, under protection against wind and rain, as opposed to commercial HiVol samplers.

Fig. S1 Scheme of sampler: 1 - adsorption trap for high volume air sampling, 2 - valve, 3 – traps for low volume air sampling, 4 and 4’ - rotameters, 5 - vacuum pump

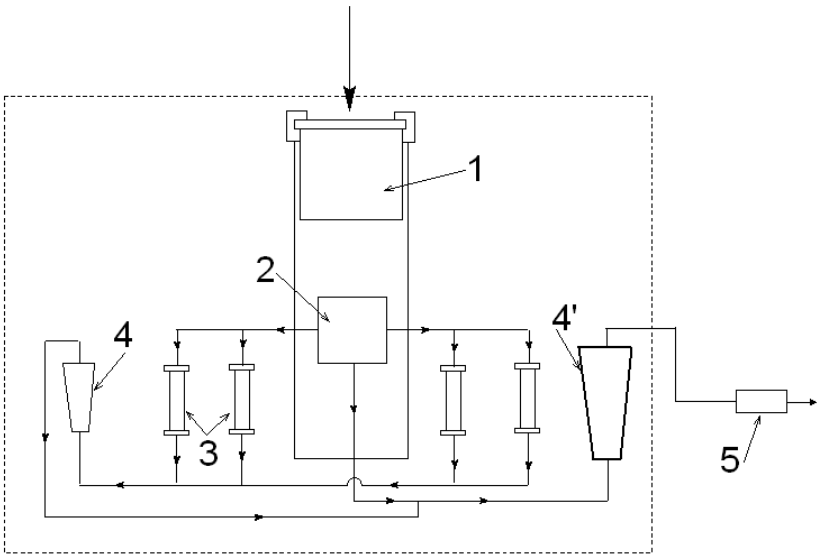

Table S1 The nomenclature of alkyl nitrates and the corresponding halides used for synthesis and yields of the synthesis reactions

Alkyl nitrate		**Yield (%)**
Methyl*	1C1	98
Ethyl	1C2	96
1-Propyl	1C3	97
1-Butyl	1C4	96
2-Butyl*	2C4	98
1-Pentyl	1C5	96
2-Pentyl	2C5	92
3-Pentyl	3C5	96
1-Hexyl	1C6	95
1-Heptyl	1C7	98
1-Octyl	1C8	99
1-Nonyl	1C9	97

* - synthesized from RI; all the others from RBr

Analytical methodology

The small amounts of adsorbents in Tenax TA® sampling makes Soxhlet extraction the most adequate. The extraction efficiency has been checked by spiking 8 g Tenax TA® with 10 µL aliquots of a reference mixture containing all the ANs in acetone at a concentration of 50 µg mL^{-1}. The recovery values for extraction of the reference compounds using the described method ranged from 85% for 1C3 to 95% for 1C9. In contrast, the large gas trap containing 100 g silicagel needed another extraction method. Specifically, the adsorbent is flushed with 400 mL of pentane and dichloromethane in a glass cooled column. The extraction efficiency was determined in the same way as for the Tenax TA® and yielded a recovery of 93 to 97 % for silicagel. Solvent desorption after adsorptive sampling combines the advantages of multiply injections with various detection methods in GC, including in sample pre-separation to reduce the complexity of the analytes (Luxenhofer et al. 1996).

In spite of the selective elution applied for silicagel, or the cleaning procedure applied to Tenax TA® after extraction, the materials still contained significant amounts of trace contaminants. However, the species selectivity of the applied GC-MS method was sufficiently high to avoid further pre-cleaning. For quantification, the mass chromatogram at *m/z* 46 is the best compromise between specificity and intensity. The calibration fits for the intensity (area) ratios as a function of the relative abundance of the ANs to 2-fluorotolune is linear over 1.5 orders of magnitude, while the precision with 5 replicate injections is within 6 % and the LOD is around 30 pg injected (cf. Table S2). A substantial difference in sensitivity for each alkyl nitrate analogue has been noticed, requiring separate calibration curves to be constructed.

The instrumental LODs and LOQs were assessed by diluting standard solutions and injecting three replicates of 1 µL of each reference mixture into the GC. The concentration giving a signal 3-time higher than the background (noise) value was considered as the minimum amount the instrument can detect. The instrumental LOQ was considered with the most diluted standard solution, which could be plotted in the calibration curve, corresponding to 3.33LOD. For the calculation of the method LOQs, the volume of the air sampled for the analysis was also taken into account.

Samples with a level below LOQ were assigned a value of (1-p)xLOQ, with “p” being the proportion of measurements with levels below LOQ (Voorspoels et al. 2002).

Table S2 Analytical performance of the GC-MS method for the study alkyl nitrates

	1C3	2C4	1C4	3C5	2C5	1C5	3C6	2C6	1C6	1C7	1C8	1C9
S	1.322	1.092	1.590	0.312	0.522	0.877	0.287	1.328	0.815	0.672	0.550	0.402
r^2	0.9996	0.9996	0.9991	0.9992	0.9989	0.9998	0.9988	0.9990	0.9997	0.9996	0.9992	0.9989
Instrumental LOD (pg injected)	18	17	14	42	29	10	17	10	11	6	10	11
Instrumental LOQ (pg injected)	56	53	45	133	92	33	55	31	34	17	30	35
Method LOD (pptv)	0.003	0.002	0.002	0.005	0.003	0.001	0.002	0.001	0.001	0.001	0.001	0.001
Method LOQ (pptv)	0.008	0.007	0.006	0.015	0.01	0.004	0.006	0.003	0.004	0.002	0.003	0.003
Precision (%), n=5 (0.5 µg mL^{-1})	1.9	1.9	0.9	6.2	4.3	2.3	6.0	3.1	2.7	2.0	3.5	1.9

S – slope of the calibration graph, r – correlation coefficient of calibration, LOD – limit of detection, LOQ – limit of quantification, n – number of replicate determinations.

Table S3 Correlation of alkyl nitrates with inorganic species and meteorological conditions

AN	Season	
	Winter-spring	**Midsummer**
1C3	-	-
2C4	-	-
1C4	HNO_2, fine Cl^-, 3C5, 1C5, 2C6, 1C7, 1C9, T_{air}(a), RH(a)	medium-NH_4^+/SO_4^{2-}/K^+, fine-Mg^{2+}, 3C5, 2C6, 1C6, 1C7, 1C9, rain
3C5	HNO_2, medium-NH_4^+, coarse-NH_4^+(a), medium-Mg^{2+}(a), 1C5, 2C6, T_{air}(a), RH(a), WS(a)	medium-NH_4^+/SO_4^{2-}/K^+, fine-Mg^{2+}, 2C5(a), rain

2C5	medium&fine-NH_4^+/NO_3^-/SO_4^{2-}/K^+, T_{air}(a), WS	coarse-K^+/Mg^{2+}, medium-SO_4^{2-}/NO_3^-/Na^+, fine-NO_3^-/SO_4^{2-}/Na^+/Cl^-, 1C5, 2C6, 1C6, 1C7, T_{air}(a), P_{air}, WS(a)
1C5	fine-Cl^-, 2C6, 1C7, 1C9	2C6, 1C6, 1C7, 1C8
3C6	-	-
2C6	HNO_2, medium-NH_4^+/NO_3^-/SO_4^{2-}, 1C6, 1C7, rain-NO_3^-, P_{air}	coarse-K^+, 1C6, 1C7, 1C8
1C6	HNO_2, medium-NH_4^+/NO_3^-/SO_4^{2-} /Ca^{2+}/Mg^{2+}/K^+,	1C7, 1C8, 1C9
1C7	HNO_2, 1C8	coarse-Na^+/K^+/Mg^{2+}, 1C8, 1C9
1C8	coarse-NH_4^+,	HNO_3, 1C9
1C9	medium-NO_3^-(a)	fine-NO_3^-/K^+,

Note: (a) – anti-correlation; the fine, medium, and coarse aerosol fractions correspond to aerodynamic diameter ranges of 0.17-0.84, 0.84-4.2, and >4.2 μm, respectively.

Table S4 Results of PCA for 2006 winter-spring

	Rotated Component Matrix[a]									
	L1	L2	L3	L4	L5	L6	L7	L8	L9	L10
HNO_2	-0.154	-0.032	0.076	0.159	0.342	-0.035	0.083	0.003	**0.654**	0.277
HNO_3	0.061	0.163	0.016	0.154	-0.060	-0.089	**0.538**	-0.053	0.372	-0.302
NH_3	-0.060	-0.043	-0.093	-0.048	-0.104	-0.066	0.075	0.026	**0.794**	-0.055
Coarse NO_3^-	0.122	-0.018	0.305	-0.146	-0.055	-0.136	0.172	**0.695**	-0.283	-0.157
Coarse NH_4^+	-0.005	-0.080	**0.832**	-0.070	-0.026	-0.019	0.265	0.187	-0.251	-0.035
Coarse SO_4^{2-}	0.373	-0.022	**0.851**	-0.094	0.069	0.058	-0.086	0.013	-0.090	-0.093
Coarse Cl^-	**0.829**	-0.147	0.306	-0.117	-0.177	0.151	0.125	-0.053	-0.110	-0.023
Coarse Na^+	**0.649**	-0.036	**0.632**	-0.074	-0.097	0.151	0.142	-0.061	-0.039	-0.020
Coarse K^+	0.145	0.064	**0.873**	-0.079	-0.089	0.147	-0.093	-0.021	0.077	0.015
Coarse Mg^{2+}	**0.853**	-0.086	0.179	-0.036	-0.078	-0.007	-0.049	0.341	-0.144	0.028
Coarse Ca^{2+}	**0.796**	-0.023	0.063	-0.034	0.013	-0.086	-0.074	**0.476**	-0.088	0.078
Medium NO_3^-	-0.220	0.236	-0.013	0.170	**0.857**	-0.069	-0.031	-0.025	-0.005	-0.013
Medium NH_4^+	-0.312	0.166	-0.016	0.341	**0.791**	-0.106	0.025	0.028	0.091	0.105
Medium SO_4^{2-}	0.002	0.148	-0.017	0.281	**0.829**	-0.097	-0.023	0.105	-0.024	-0.157
Medium Cl^-	**0.676**	-0.148	-0.082	-0.183	-0.092	0.159	-0.127	-0.227	0.217	-0.168
Medium Na^+	**0.706**	-0.052	0.204	-0.143	0.101	0.010	**0.444**	-0.067	-0.098	-0.091
Medium K^+	0.114	**0.892**	0.033	-0.033	-0.035	-0.033	0.053	-0.022	0.080	-0.007
Medium Mg^{2+}	0.186	-0.152	-0.017	-0.206	**0.812**	0.009	0.006	0.073	-0.001	0.036

Medium Ca^{2+}	0.301	-0.029	0.039	-0.080	0.220	-0.134	0.038	**0.644**	0.077	0.233
Fine NO_3^-	-0.305	**0.699**	-0.108	-0.053	0.143	-0.051	-0.384	-0.189	0.038	0.252
Fine NH_4^+	-0.365	**0.738**	-0.069	-0.002	0.186	-0.102	-0.329	0.036	-0.025	0.213
Fine SO_4^{2-}	-0.140	**0.787**	-0.044	-0.064	0.183	-0.114	-0.077	0.341	-0.133	0.074
Fine Cl^-	0.005	0.160	**0.485**	-0.056	-0.101	0.100	-0.653	-0.008	0.284	-0.079
Fine Na^+	0.076	0.340	**0.667**	0.028	0.103	-0.056	-0.348	0.097	0.137	0.020
Fine K^+	-0.103	**0.805**	0.320	-0.109	0.023	0.078	0.000	-0.030	0.040	-0.051
Fine Mg^{2+}	-0.061	0.133	-0.005	-0.041	0.034	-0.145	-0.592	-0.055	-0.238	-0.164
Fine Ca^{2+}	-0.063	0.108	-0.078	-0.011	-0.042	-0.037	0.026	-0.049	0.047	**0.803**
1C4	0.072	-0.097	0.101	-0.011	-0.152	**0.914**	-0.095	-0.004	-0.022	0.069
3C5	0.076	0.038	-0.094	0.199	0.045	**0.651**	0.138	-0.139	0.114	-0.158
2C5	-0.015	**0.597**	-0.057	-0.011	0.051	0.340	0.389	-0.069	-0.179	-0.220
1C5	0.035	-0.116	0.125	-0.021	-0.137	**0.927**	-0.081	0.012	-0.060	0.064
2C6	-0.078	-0.031	-0.075	**0.934**	0.093	0.085	0.062	-0.118	0.008	0.027
1C6	-0.124	-0.089	-0.076	**0.940**	0.149	0.074	0.039	-0.059	0.024	-0.056
1C7	-0.122	-0.097	-0.072	**0.957**	0.117	-0.017	0.011	-0.052	0.027	0.009
1C8	0.116	-0.135	0.089	0.100	-0.050	-0.138	0.139	-0.554	-0.271	0.200
1C9	0.030	0.374	0.137	-0.006	0.052	**0.636**	0.286	0.019	-0.218	-0.089
Eigenvalue (total)	6.962	4.681	3.457	3.306	2.383	1.814	1.751	1.577	1.393	1.127
Variance (%)	19.338	13.004	9.604	9.183	6.618	5.039	4.863	4.381	3.870	3.129
Cumulative (%)	19.338	32.341	41.945	51.128	57.747	62.876	67.649	72.030	75.901	79.030
Major source	sea spray	biomass burning	secondary aerosol	photochem. from HCs	diesel emission	marine emission	local combustion	local background	animal farming	unidentified local source

[a] – rotation converged in 14 iterations; Note: L1, L2, etc. stands for “loading on Component 1”, “loading on Component 2”, and so on.

Table S5 Results of PCA for 2006 summer

	Rotated Component Matrix[a]								
	L1	L2	L3	L4	L5	L6	L7	L8	L9
HNO_2	0.009	-0.213	-0.154	-0.133	0.017	**0.558**	-0.352	0.094	-0.273
HNO_3	0.399	0.101	-0.117	-0.217	-0.100	-0.026	-0.013	**0.688**	-0.023
NH_3	0.165	-0.052	0.008	0.140	0.026	0.000	-0.047	-0.019	**0.883**
Coarse NO_3^-	0.195	0.219	0.035	-0.045	-0.021	**0.413**	**0.680**	0.334	-0.051
Coarse NH_4^+	0.034	0.099	**0.821**	0.060	0.189	0.272	-0.058	-0.178	0.090
Coarse SO_4^{2-}	0.097	0.033	0.049	0.078	0.142	0.086	**0.933**	0.002	0.008
Coarse Cl^-	0.107	-0.101	0.168	-0.012	-0.103	-0.213	**0.838**	-0.257	-0.058
Coarse Na^+	0.098	-0.048	**0.822**	0.116	-0.082	-0.119	0.206	-0.359	0.053
Coarse K^+	0.118	-0.073	**0.463**	-0.007	-0.151	0.071	0.097	-0.571	0.015
Coarse Mg^{2+}	0.008	0.013	**0.936**	0.170	-0.053	-0.159	0.083	-0.049	0.015
Coarse Ca^{2+}	-0.059	-0.067	**0.884**	0.170	-0.023	-0.009	0.046	0.198	-0.114
Medium NO_3^-	0.051	0.259	0.111	0.175	-0.030	**0.700**	0.391	-0.131	-0.211
Medium NH_4^+	-0.097	0.180	0.089	-0.109	**0.505**	**0.575**	-0.184	0.036	0.275
Medium SO_4^{2-}	-0.073	0.290	-0.027	0.057	**0.569**	**0.620**	0.207	-0.122	0.151
Medium Cl^-	-0.016	-0.075	-0.256	**0.925**	-0.026	-0.052	0.054	-0.101	-0.030
Medium Na^+	-0.015	0.024	0.324	**0.844**	0.024	0.065	0.124	-0.216	-0.020
Medium K^+	0.176	0.057	0.054	0.078	0.733	0.290	-0.143	0.306	0.088
Medium Mg^{2+}	-0.100	-0.055	0.203	**0.906**	-0.032	-0.096	-0.001	0.024	0.159

Medium Ca^{2+}	-0.091	-0.073	0.337	**0.897**	-0.026	0.038	-0.076	0.086	0.069
Fine NO_3^-	-0.041	**0.964**	-0.088	-0.040	-0.040	0.075	0.033	-0.005	0.014
Fine NH_4^+	0.000	**0.639**	0.008	-0.134	0.057	**0.539**	-0.081	0.262	0.175
Fine SO_4^{2-}	-0.016	**0.572**	-0.093	-0.070	0.170	**0.597**	0.122	-0.165	0.180
Fine Cl^-	-0.030	**0.942**	-0.001	0.008	-0.021	-0.071	0.118	-0.002	-0.098
Fine Na^+	0.002	**0.980**	0.028	-0.033	-0.031	0.041	0.021	-0.017	-0.047
Fine K^+	-0.032	**0.719**	-0.051	-0.075	-0.097	0.293	-0.121	0.110	0.200
Fine Mg^{2+}	-0.067	**0.915**	-0.011	-0.012	0.280	-0.061	0.054	-0.011	-0.105
Fine Ca^{2+}	-0.120	**0.902**	0.098	0.006	-0.039	0.121	-0.011	0.082	-0.035
1C4	-0.046	-0.042	-0.033	-0.048	**0.956**	-0.012	0.068	-0.081	-0.050
3C5	-0.043	-0.046	-0.037	-0.045	**0.969**	-0.016	0.054	-0.040	-0.037
2C5	**0.876**	-0.045	0.027	0.005	-0.008	-0.004	0.172	-0.140	0.133
1C5	**0.936**	-0.073	-0.001	-0.065	-0.023	-0.028	0.059	0.118	-0.023
2C6	**0.994**	-0.038	0.005	-0.037	0.004	-0.003	0.014	0.040	0.018
1C6	**0.991**	-0.033	0.032	-0.023	0.007	0.003	0.047	0.026	0.013
1C7	**0.993**	-0.024	0.020	-0.019	0.015	0.017	0.023	0.015	0.015
1C8	**0.880**	-0.096	-0.022	-0.094	-0.056	-0.021	0.028	0.275	0.035
1C9	**0.973**	0.005	0.040	0.008	0.028	0.029	0.019	-0.098	0.029
Eigenvalue (total)	7.220	6.623	4.998	3.496	2.547	2.307	1.718	1.306	1.044
Variance (%)	20.057	18.396	13.884	9.711	7.075	6.409	4.772	3.627	2.900
Cumulative (%)	20.057	38.453	52.337	62.048	69.122	75.532	80.304	83.931	86.831
Major source	photochem. from HCs	fossil fuel burning	resuspended dust	sea salt	biomass burning	secondary aerosols	regional/coastal background	local traffic	animal farming

[a] – rotation converged in 8 iterations; Note: L1, L2, etc. stands for “loading on Component 1”, “loading on Component 2”, and so on.

Reference for Supplementary Information Section

Voorspoels, S., Covaci, A., Maervoet, J., & Schepens, P. (2002). Relationship between age and levels of organochlorine contaminants in human serum of a Belgium population. *Bulletin of Environmental Contamination and Toxicology*, 69(1), 22-29.